

A Two-Stage Detector For First-Order Sea Clutter In Hf Surface Wave Radar

Ha Huy Dung^{1,*}, Ph.D. Le Duy Hieu¹, Ph.D. Bui Ngọc My², Cao Viet Linh¹

¹ Radar institute, 17 Hoang Sam Street, Ha Noi, Viet Nam.

² Department of Education and Training, Academy of Military Science and Technology, 17, Hoang Sam Street, Ha Noi, Viet Nam.

Abstract:

The detection capabilities in vertical polarized, High-frequency Surface Wave Radar (HFSWR) are limited by the clutter spikes in first-order sea clutter. The energy, position, and Doppler frequency of first-order sea clutter depend on the sea states, which are non-homogeneous — because of that, using a fixed expression to eliminate sea clutter gives limited results. In this paper, the authors proposed a new adaptive method using a two-stage detector based on the Order Statistic Constant False Alarm Rate (OS-CFAR) principle. The approach shows the capability to eliminate heterogeneous and detect targets in the vicinities of sea clutter in the Range – Doppler map.

Key words: high frequency, surface wave radar, noise, sea clutter, adaptive CFAR.

1. Introduction: Sea clutter in the HF range is caused by the interaction between electromagnetic waves and ocean waves [1-2]. The first-order sea clutter is generated by ocean waves that are half the operating wavelength λ_0 of the radar, consisting of two peaks with high energy corresponding to the direction of movement towards or away from the radar. The spectrum of the first-order sea clutter depends

on the resonant frequency and the sea current. According to [3], the Doppler frequency, f_{Br1} , of first-order sea clutter is calculated as:

$$f_{Br1} = \pm \sqrt{\frac{g}{\pi\lambda_0}} \quad (1)$$

In the presence of sea current, the Doppler frequency is expressed as follows [2], [5-6]:

$$f_{Br1} = \pm \sqrt{\frac{g}{\pi\lambda_0}} - \frac{2V_c}{\lambda_0} \cos \alpha \quad (2)$$

where: $g = 9.81 \text{ m/s}^2$ is the gravitational acceleration, V_c is the flow rate, and α is the angle between the flow direction and the beam angle of the radar.

The remaining component of sea clutter is called second-order sea clutter with energy peaks located at the harmonics of the f_{Br1} frequency, which is difficult to observe but has a minimal impact, so we can ignore them.

The detector in HFSWR uses the constant false alarm rate (CFAR) principle. This method is based on the Neyman-Pearson lemma, aiming to maximize target detection with a given false alarm rate. The detection threshold is determined by the false alarm rate [7]. Due to the high energy of the first-order sea clutter, which often masks the targets in the vicinity, traditional CFAR techniques usually do not guarantee the detection quality in the HFSWR. In recent years, solutions to implement CFAR in HFSWR have been studied in the direction of adaptation. The main research directions and their limits include:

- + Presegmentation-based adaptive CFAR [8]: This method changes the reference window's size to suppress clutter. This solution is limited by the inability to determine the clutter regions to perform an adaptive reference window. Also, the window size values do not guarantee the optimality when the clutter characteristics cannot be described mathematically;

- + Adaptive CFAR method according to environmental aspects [9-10]: Each CFAR technique has certain advantages for different operating environment properties. Therefore, applying a specific CFAR technique to one particular environment will improve the quality of the detector. However, it's difficult to determine the environment properties to use the correct CFAR method for the sensor in practice.

- + Adaptive power regression thresholding [11]: This method reduces the energy fluctuations of clutter spikes relative to targets nearby, thus reducing the impact of the high-energy clutter domain on the average noise level. This is a support solution for CFAR techniques, but it is not an adaptive CFAR.

+ Adaptive solution using global knowledge of sea clutter-dominated regions [4], [8]: Studies using available features of clutter spikes are two-stage detectors. In the published studies, two main development directions, including Detect/eliminate clutter spikes using traditional CFARs, use the target's correlation in neighboring radar cells.

These adaptive CFAR solutions provide certain results and aim to eliminate the heterogeneous clutter in HFSWR. There are, however, still problems such as the incomplete application of the first-order sea clutter model, using mathematical transformations that change the probability distribution function properties of the signals. These drawbacks lead to the instability of the detection itself. Therefore, the optimization and suitability of CFAR solutions applied to HFSWR is always an open study direction.

The paper proposes an adaptive, two-stage CFAR (TSA-CFAR) based on order static CFAR (OS-CFAR) and the characteristics of first-order sea clutter. The difference of this new approach is the detection process doesn't require knowledge beforehand of the Doppler frequency f_{Br1} for first-order sea clutter. Section 2 describes the detection principle, and Section 3 presents the simulation results and performance analysis for this detector.

2. Two-stage cfar detector. The study is done using a simulated HFSWR station operating at a frequency of 3.5Mhz with a Linear Uniform Array (ULA) consisted of 32 antenna elements. The processing in the HFSWR is carried out through the received signal transformation stages to construct a data matrix in two dimensions, Range and Doppler, or an RD map. After receiving the RD map, the detection processing will be carried out [12]. The proposed TSA-CFAR detector consists of two processing stages:

+ Stage 1: We use three sets of OS-CFAR in parallel, including one original OS-CFAR with Cell Under Test (CUT) in the middle of the reference window [13], two OS-CFARs with CUT located at the left and right borders of the reference window, respectively. Target detection results are determined when any of the three OS-CFARs confirms the target's existence in CUT. The OS-CFAR technique was chosen because of its good performance in the case of many closely positioned targets, and its parameter set is highly customizable during operation. Unlike typical radars with false alarm rates lower than 10^{-5} , in HFSWR, the P_{FA} value is usually in the range of 10^{-4} to 10^{-3} . According to [13], the calculation for P_{FA} as a function of detector parameters is described as:

$$P_{FA} = k \binom{N}{k} \frac{(k-1)!(T_{OS}+N-k)!}{(T_{OS}+N)!} \quad (3)$$

where: T_{os} is the fixed detection threshold; N is the reference window size; N is the noise assessment position after the reference cells have been ranked based on their energy level. It can be seen that with a selected P_{fa} , there will be many usable sets of N , k , T_{os} values.

This approach uses three sets of OS-CFAR simultaneously to detect all targets, especially those located in the energy spike areas or two targets located too close to each other. In a homogenous environment, it's easy to detect a target using the set of 3 OS-CFARs. When a target is masked because its energy is below the detection threshold in one OS-CFAR detector, it will be detected in the other CFAR, which ranks the cells in the opposite direction. A sensor using a combination of 3 OS-CFARs, as illustrated in Figure 1, will not miss any targets, and we only use one type of CFAR detector. Also, all sea clutter information will be detected as well after the first stage of the TSA-CFAR.

The second stage of TSA-CFAR uses the following criteria to detect first-order sea clutter [2]:

- + First criterion: The first-order sea clutter that appears will spread in a large range area;
- + Second criterion: The first-order sea clutter has a two-line spectral form in the negative and positive Doppler frequency domains, $D_x + \Delta x$ and $D_y + \Delta y$.

The first-order clutter filtering steps are performed as follows:

+ Step 1: Determine the Doppler frequency, which can possibly be first-order sea clutter: From the range-doppler map data in the matrix form of $N_R \times N_D$ with N_R , N_D is the number of range cells and Doppler cells, respectively. Each Doppler frequency in the RD map is a vector with N_R range cells. The vectors corresponding to $D_x + \Delta x$ and $D_y + \Delta y$ will be checked in the range dimension for the presence of possible clutter. D_x is the negative Dopplers. The central frequencies D_x , D_y are calculated using (1), (2) and rewritten as (4):

$$\begin{cases} D_i = -\sqrt{\frac{g}{\pi\lambda_0}} - A \frac{2V_c}{\lambda_0} \cos \alpha \\ D_j = \sqrt{\frac{g}{\pi\lambda_0}} - A \frac{2V_c}{\lambda_0} \cos \alpha \end{cases} \quad (4)$$

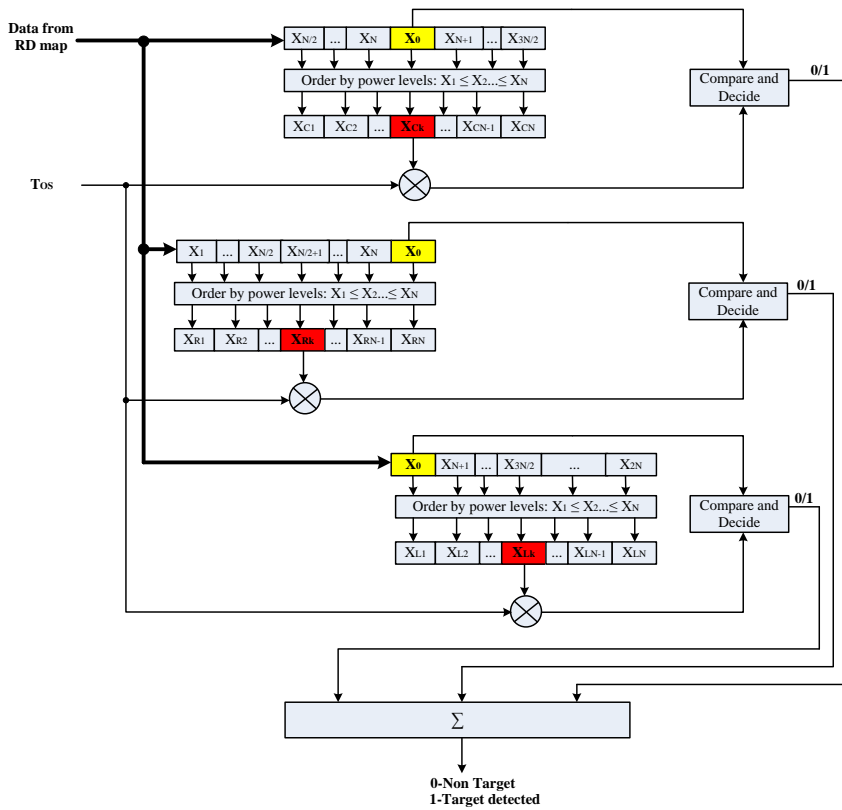


Fig 1. The architecture of a TSA-CFAR detector.

A will be zero when there is no sea current, and it will be 1 when sea current presents.

Subtract two equations to eliminate the uncertainty of the sea current, obtained D_y as in (5) corresponds to each value D_x is checked.

$$D_y = 2 \sqrt{\frac{g}{\pi \lambda_0}} - D_x \quad (5)$$

The criteria for determining the frequency pair as the spectrum of first-order sea clutter is the number of range cells that exist target detection at $D_x + \Delta x$ and $D_y + \Delta y$ must both exceed a pre-selected threshold.

+ Step 2: The frequencies in the RD map are likely to be the spectrum of first-order sea clutter will be further evaluated using the following condition: the number of consecutive detected range cells in the

suspected frequency exceeds a pre-selected threshold. Any detections that meet this condition will be eliminated.

The final result left only the target markers, and all first-order sea clutter regions are eliminated. The implementation of the TSA-CFAR using Matlab simulated data is presented and evaluated in the next section.

3. Performance assessment of TSA-CFAR in HFSWR. To evaluate the detector's performance, we generate a simulation database for an HFSWR system consisted of 32 uniform linear array antenna elements with a carrier frequency of 3.5Mhz. We generated ten targets in the presence of first-order sea clutter. The targets are positioned close to each other and close the clutter regions. The first-order sea clutter is generated with the followings parameters:

- + In the range between 0÷50km, there is no sea current. The wind direction is 60^0 relative to the beam direction.
- + In the range between 50÷80km, there is no sea current. The wind direction is 0^0 relative to the beam direction.
- + In the range between 80÷250km, the sea current presents with a wind velocity of 2m/s. The wind direction is of 60^0 relatives to the beam direction.

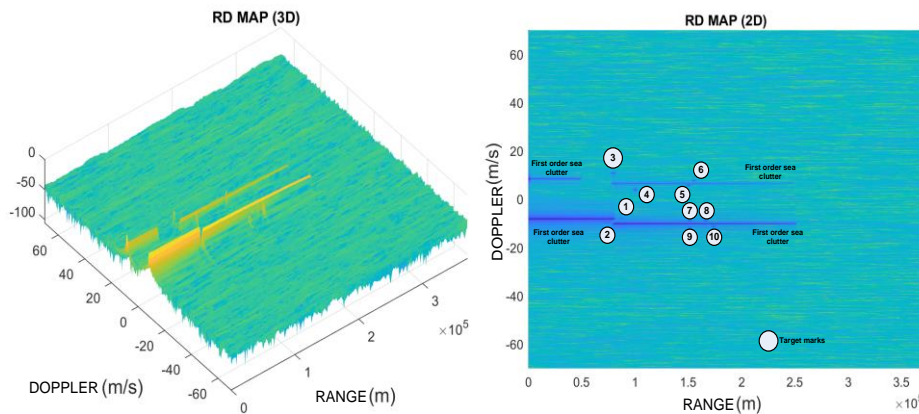


Fig 2. Simulated RD Map in HFSWR

After filtering and FFT processing, the received signals are presented in the form of a Range-Doppler Map, illustrated in Figure 2. Figure 2b) is the 2D view, provided us with the information of ranges, velocities of the targets, and first-order sea clutter region as we can see that the sea clutter can appear randomly, not just in the symmetrical form.

In HFSWR, sea clutter energy typically amounts to 33% of the energy values sorted by OS-CFAR[14], along with the spreading spectrum characteristic of information processing through Fast Fourier Transform (FFT), the N , k , and T_{os} set will differ from the relationship in equation (3). We investigated the $[N, k, T_{os}]$ and selected the sets that meet the detection requirements, which are:

[12;6;4], [12;8;3], [12;8;4], [12;9;3], [12;9;3], [16;8;4], [16;8;5], [16;8;6], [16;10;3], [16;10;4], [16;10;5], [16;12;3], [16;12;4], [16;12;5], [24;8;7], [24;8;8], [24;8;9], [24;8;10], [24;12;4], [24;12;5], [24;12;6], [24;12;7], [24;16;5], [24;16;6], [24;18;3], [24;18;4], [24;18;5], [24;18;6], [32;16;3], [32;16;4], [32;16;5], [32;16;6], [32;16;7], [32;16;8], [32;16;9], [32;21;3], [32;21;4], [32;21;5], [32;21;6], [32;24;3], [32;24;4], [32;24;5], [32;24;6], [32;24;7].

From the results, we can see that:

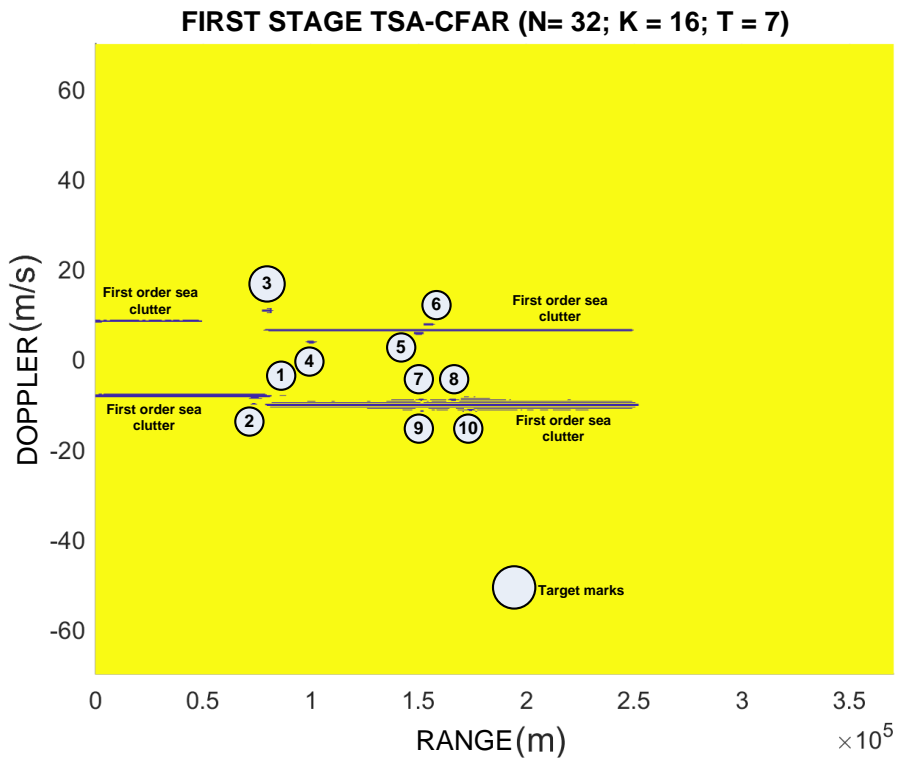
+ First, all N that is smaller or equal to 8 are not suitable to use in HFSWR because of the spectrum spreading phenomenon that happens in FFT for target and clutter signals;

+ Second, the (N, k, T) relation closely follows formula (3), as expected with an OS-CFAR. However, the k, T relation is somewhat different because the CUT's position can sometimes be in the spectrum spreading of the target. If we chose T according to (3), the threshold would be higher than the target's energy level, thus detecting it.

+ Third, $k \leq 3N/4$. This is consistent with the statistical estimates of the clutter energy in HFSWR systems.

+ Fourth, the TSA-CFAR offers flexibility when choosing the parameter sets. This ensures the practical application of the proposed solution.

Next, we will present the results of the detecting process in TSA-CFAR with the parameter set: $N = 32, k = 16; T = 7$.



(a)

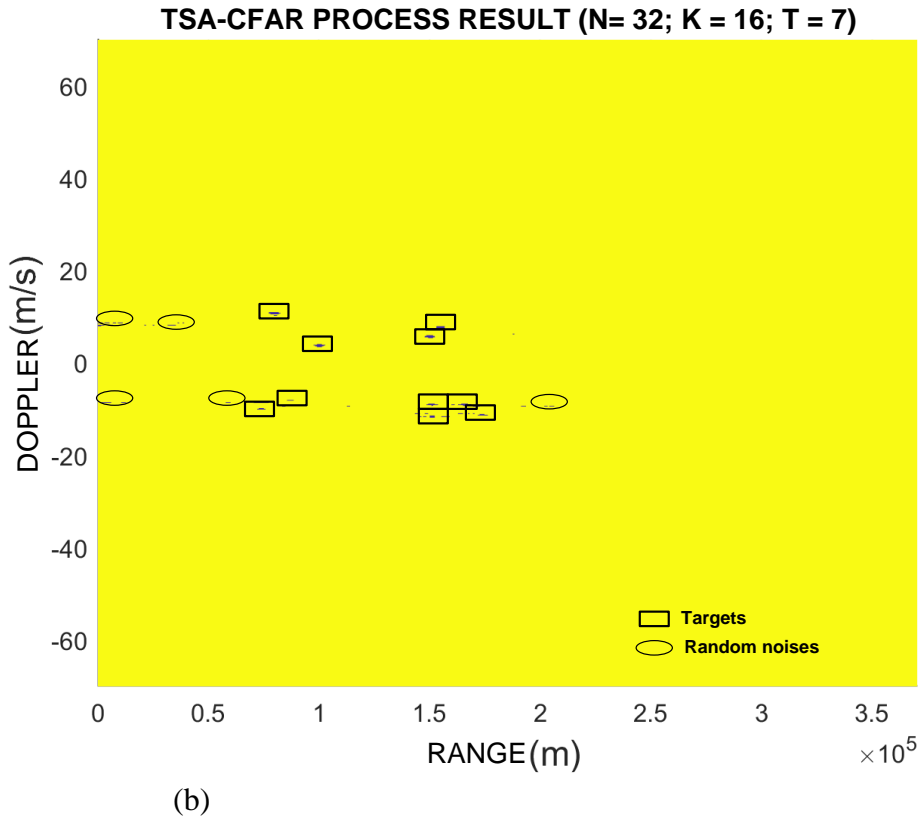


Fig 3. Detection results in TSA-CFAR for the first stage and second stage

Figure 3a) presents the detection results using a combination of 3 OS-CFARs in the first stage of the TSA-CFAR.

After the first stage of the TSA-CFAR, all targets present in the detection map. And the first-order sea clutter region also presents showing its symmetric two-line spectral form. Using these criteria, in the second stage, the TSA-CFAR implements the algorithm described in Section 2 to eliminate all unwanted clutter. The filter criteria as follows:

- + Spectrum spreading factor $\Delta D = 8$;
- + Detection factor for possible first-order sea clutter $TC1 = 20$;
- + Threshold to eliminate clutter $TC2 = 8$;

The final results are presented in Figure 3b. We can see that the clutter is eliminated, leaving the real targets without missing any information. There are still some detection marks on the map. They are random noise that can be further eliminated using correlation processing or tracking processing.

To further demonstrate the advantage of this approach, Figure 4 presents the detection results of the traditional OS-CFAR and Variability Index CFAR (VI-CFAR) [10] as a comparison. Figure 4(a) presents the detection results of a single OS-CFAR. As we can see, the traditional OS-CFAR can not detect the targets in the vicinity of the clutter edge (target No2). It also presents the clutter edges as false targets. Detections like that can be challenging to differentiate from real targets. In Figure 4(b), the VI-CFAR can not eliminate all the sea clutter, and the detection of targets adjacent to the clutter region is unstable.

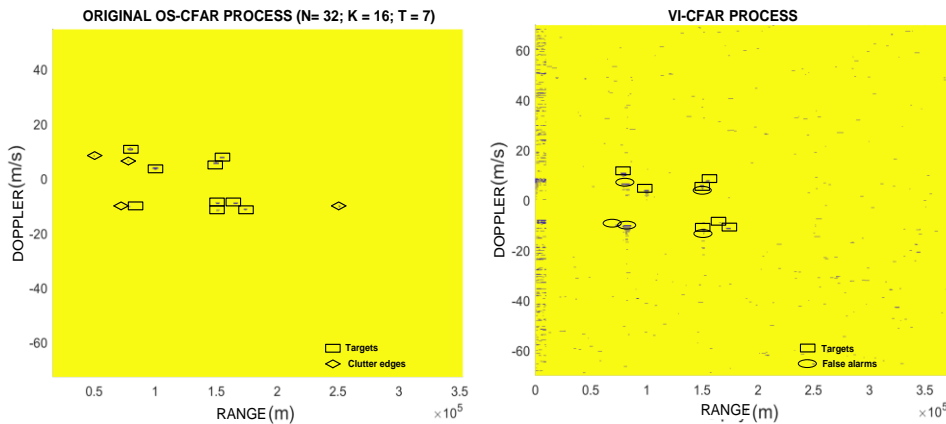


Fig 4. Detection results using cell averaging CFAR methods

4. Conclusion. HFSWR's heterogeneous operating environment has set the requirement for the use of highly adaptive CFAR detectors. Recently, the research on adaptive CFAR has had clear feasibility directions. There are development directions such as: adapting the reference window shape, switching of CFAR types according to the environmental properties, etc., or a two-stage detector using the characteristics of first-order sea clutter. Based on the CFAR technique and the shortcomings of the previous studies, the paper proposed a solution to construct a two-stage TSA-CFAR detector. Stage one uses order static CFAR to take advantage of the ability to detect closely placed targets while also highlighting the

spectrum of first-order sea clutter instead of only remove a part of the clutter. Phase two will filter out the noise position according to clutter characteristics. The authors presented the structure of the detector and evaluated its performance using simulation data by comparing it with other approaches. The simulations showed that the TSA-CFAR solution has a high target detection probability and can mitigate the target masking phenomenon when two targets are closely placed together.

Noted that the TSA-CFAR does not detect targets whose velocity coincides with the spectrum of the first-order sea clutter and the ranges inside the sea clutter area (blind area). Because to perform target detection in the blind area, it is necessary to use other support solutions such as in [3] or frequency hopping combined with adjusting the radiation pattern. The future work includes surveying and evaluating the detection ability and studying the method of parameter correction for a two-stage detector to have a small effective reflectance area, and research on the construction a full model of the HFSWR signal types based on actual data usage.

References

- [1] Sevgi, L., Ponsford, A., Chan, A (2001) An integrated maritime surveillance system based on high frequency surface wave radars, Part 1 - Theory of operation”, IEEE Proc. Ant. And Prop., 43.
- [2] Ponsford, A., Sevgi, L., Chan, A (2001) An integrated maritime surveillance system based on high frequency surface wave radars, Part 2 - Operational status and system performance, IEEE Proc. Ant. And Prop., 43.
- [3] Ponsford, A. M., Wang, J., (2010) A review of high frequency surface wave radar for detection and tracking of ships”, Turkish Journal of Electrical Engineering and Computer Sciences.
- [4] Gupta, A. (2015) Theory and Measurement Validation of Novel HFSWR Receiver Architecture: Antenna Design, Clutter Suppression and Detection, Department of Electrical Engineering of Helmut Schmidt University, Germany, pp. 80-100.
- [5] Wang, Y., Mao, X., Zhang, J., Ji, Y., (2018) Detection of Vessel Targets in Sea Clutter Using In Situ Sea State Measurements With HFSWR, IEEE Geoscience and Remote Sensing Letters.
- [6] Xie, J., Ji, Z (2013) First order ocean surface cross-section for shipborne HFSWR, Electronics letters, 49(16).

- [7] Xiaoli, L (2009) Enhanced Detection of Small Targets in Ocean Clutter for High Frequency Surface Wave Radar, A Dissertation Submitted in Partial Fulfillment of the Requirements for the Degree of Doctor of Philosophy in the Department of Electrical and Computer Engineering, 67-87.
- [8] Hinz, J.O., Holters, M., Zölzer, U., Gupta, A et al. (2012) Presegmentation-based adaptive CFAR detection for HFSWR, IEEE Radar Conference.
- [9] Mashade, M. B. EL (1995) Analysis of the censored-mean level CFAR processor in multiple target and nonuniform clutter, Radar, Sonar and Navigation, IEE Proceedings, **142**(5), 259 -266.
- [10] Cheeseman, A. (2017) Adaptive Waveform Design and CFAR Processing for High Frequency Surface Wave Radar, Graduate Department of The Edward S. Rogers Sr. Department of Electrical & Computer Engineering University of Toronto.
- [11] Dzvonkovskaya, A., Rohling, H (2006) Target detection with adaptive power regression thresholding for HF radar, International Conference on Radar.
- [12] Stojkovic, N., Nikolic, D., Petrovic, P., Tomic N et al. (2019) An Implementation of DBF and CFAR Models in OTHR Signal Processing”, IEEE 15th International Colloquium on Signal Processing & its Applications (CSPA 2019).
- [13] Richards, M. A (2015) Fundamentals of Radar system processing - second Edition, Mc Graw Hill Education, 354-360.
- [14] OTHR-ST-Specification “Part 7-Signal Processing, Detection and Tracking”, HELZEL Messtechnik 2018